

Scaling Laws and the Differential Equations of an Entrained Flow Coal Gasifier

RONALD S. KANE

Department of Mechanical Engineering
Manhattan College
Riverdale, New York 10471

and
ROBERT A. MC CALLISTER

Process Technology Department
Foster Wheeler Energy Corporation
Livingston, New Jersey 07039

A formal order of magnitude analysis was applied to the differential equations describing mass, momentum, and energy transport in an axially translating, vortex flow field and used to determine the importance of various terms. Significant dimensionless parameters, suitable for establishing scaling laws, appear naturally from the equations. Among the important parameters are the swirl number, geometric scale ratio, Froude number, and particle loading ratio. These parameters were combined to establish rules for complete similarity between a model and a prototype gasifier.

SCOPE

The entrained flow gasifier is one of four major types of coal gasifiers being considered as the starting point for the manufacture of clean fuel gas from coal. Several types of entrained flow coal gasifiers have been proposed or developed. Some of these depend primarily on axial jet mixing with one or more injection nozzles (Smoot, 1975), while others develop a vortex field. To date, very few experimental studies have been performed of the flow phenomena characteristic of an entrained flow gasifier involving particle motion in an axially translating confined vortex (Elliot et al., 1952; Smith, 1976).

As a result of Bituminous Coal Research, Inc. (BCR) studies of means to produce high Btu gas by coal gasification (Anon., 1965), a two-stage entrained flow gasifier was developed which depends upon a confined vortex field for major gasification reactions. This concept, which has been patented for the production of a methane rich fuel gas (Donath, 1974), may also be applied for the production of a clean, low British thermal unit gas suitable for gas turbine fuel. The expected capability of this type of gasifier to handle large quantities of caking coals, widely available in the United States, has led several industrial firms to build pilot plants (McCallister and Ashley, 1974; Hull, 1975; Zahradnik and Grace, 1973).

The experimental data generated by these pilot plants necessitate the development of rational data correlation techniques and scale-up procedures for use in the design of commercial size plants. Further, a systematic exposition and evaluation of the governing equations, describing the fluid and particle mechanics of the flow field, is necessary before the parallel generation of analytically derived data can proceed.

The purpose of this paper is to report the results of

an order of magnitude analysis of the governing differential equations for the flow field. Using the techniques of the order of magnitude analysis, the relative significance of various terms and phenomena can be evaluated without the necessity for a formal solution to the equations. Dimensionless groups that can be used to develop scaling criteria arise naturally from the equations themselves. These dimensionless groups can then be combined to establish rules for similarity between acceptable operation in a pilot plant and a corresponding operation in a commercial plant. Several aspects of the gasifier behavior and design are not treated in this paper. Of particular interest are the chemistry of the gasification reactions and the integration of the gasifier into the operation of a combined cycle system. These may be treated in future publications.

There is some resemblance between the equations describing the flow field in a swirling combustor and those describing the vortex flow field in the entrained flow gasifier. For several items such as the significance of the swirl number and the magnitude of the turbulent eddy viscosities, the best comparisons that can be made are to the work reported by Beer and Chigier (1972). For the entrained flow gasifier, a simple interpretation of the swirl number based on gasifier geometry is possible. This idea is in agreement with work on combustors (Beer and Chigier, 1972). The order of magnitude analysis, with some extrapolation from the behavior of linear flows (Hinze, 1959), can also be used to predict the approximate magnitude and importance of the eddy viscosity components in a swirling flow. This preliminary step to the analysis of the overall equations was necessary in order to assess the importance of common scaling parameters such as the Reynolds and Froude numbers.

CONCLUSIONS AND SIGNIFICANCE

Preliminary investigation of the flow field indicated that three basic assumptions could be made before setting down the governing differential equations: the gas flow field has circumferential symmetry; the solid particles can be described as equivalent spheres; and the gas flow can be represented by incompressible aerodynamics. The first assumption is reasonable considering the symmetry of the cylindrical system and the uniform spacing of

air, steam, and particle injection nozzles around the periphery of the lower stage of the two-stage gasifier. The second assumption is a standard one (Boothroyd, 1971) used for most analyses of particulate systems. The third assumption is valid provided gas velocities are small compared to the sonic velocity; that is, the Mach number is low. Shapiro (1953) reports negligible errors, using incompressible formulas, for Mach numbers much higher than those in the gasifier. The validity of this assumption indicated that Mach numbers need not be matched in scaling from a smaller to a larger model, provided the Mach number is lower than, say, 0.3. Use of the incompressible form of the equations of motion could

Correspondence concerning this paper should be addressed to Robert A. McCallister.

0001-1541/78/9842-0055/\$01.15 © 1978, American Institute of Chemical Engineers.

still, however, consider the effect of buoyancy forces caused by density gradients.

The order of magnitude analysis was able to reduce the lengthy partial differential equations for three dimensional swirling flow to a considerable extent. In some cases, the partial differential equations were reduced to either ordinary differential equations or to algebraic equations involving very few terms. The reduction of the equation size also reduced the number of dimensionless groups that were significant for scaling. The fact that many dimensionless groups were seen in several equations also limited the number of significant groups. One common group, the viscous Reynolds number, was found to be insignificant for scaling purposes.

The turbulent terms, Reynolds stress terms, in the governing equations for the suspending gas flow were also much more important than the viscous terms. The order of magnitude of the eddy viscosities corresponded exactly to those reported by Beer and Chigier (1972) for a swirling flow in a combustor. The largest components of the eddy viscosity tensor were the zz , $z\theta$, and $\theta\theta$ components. The values for the rz , rr , and $r\theta$ components were an order of magnitude smaller. The smallest value was for the $r\theta$ direction.

Although the turbulent terms were always more important than the viscous terms, many were in turn insignificant compared to terms describing inertial, centrifugal, Coriolis, pressure, buoyancy, gravity, or particle drag forces. These significant terms provided the dimensionless groups needed to establish the scaling criteria. Among the most important groups were the radius to length ratio, the swirl number, Froude number, particle loading ratio, local relative turbulence intensity, buoyancy-gravity force

ratio, and reaction-residence time comparison. The swirl number, defined as the ratio of circumferential momentum flux to axial momentum flux, was found to be a function of the gasifier geometry alone. It was possible to directly relate the characteristic velocities in the radial, circumferential, and axial directions through the swirl number or the geometry.

If we recognize that such scaling may not be desirable or feasible for an industrial scale system, almost complete similarity between a small scale model and a large scale prototype would be possible by the following rules derived from a combination of the significant dimensionless groups:

1. Having the same material properties in the model and the prototype.
2. Having the same particle loading ratio.
3. Increasing the gasifier length directly with the gasifier radius.
4. Having the same swirl number in the model and the prototype.
5. Increasing the axial velocity with the square root of the gasifier radius.
6. Maintaining the same particle diameter provided the particles do not deviate greatly from the conditions of Stokes flow.
7. Decreasing the reaction rate with the square root of the gasifier radius.

In an actual system, the length of the gasifier may be limited and not directly scaleable with gasifier radius. Some compromises may have to be made to accommodate the violation of geometric similarity. This should be considered after pilot plant data becomes available.

BACKGROUND

Operation of coal gasification combined cycle plants has been proposed as a method of producing power from United States coal reserves and avoiding deleterious environmental effects (McCallister and Ashley, 1974). These plants generate clean, low British thermal unit gas from coal which is used on-site as fuel for gas turbine driven electrical generators. The combined cycle also utilizes the process heat from the gasification process to generate steam for conventional steam turbine driven electrical generators. Overall, the combined cycle plant is

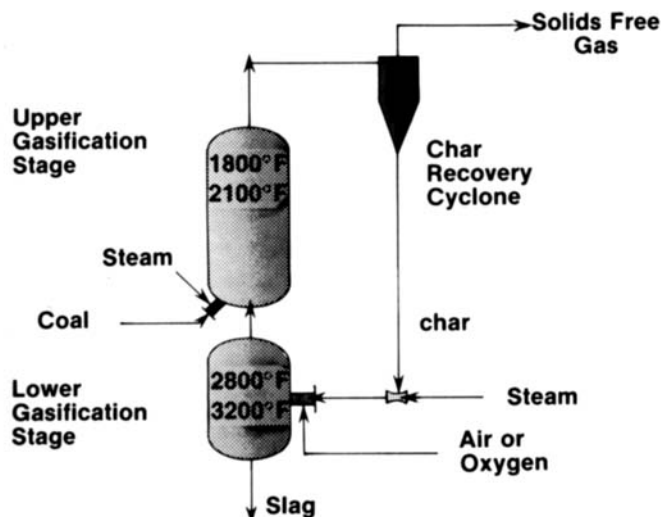


Fig. 1. Two-stage entrained flow gasifier.

capable of thermal efficiencies approaching 45%, with environmentally acceptable levels of pollutant emission and waste heat rejection.

The most important part of the combined cycle plant is the gasifier. The gasifier type considered in this paper operates in two stages as an entrained flow unit in a pressure range of 1.38 to 10.34 MPa (200 to 1500 lb/in.² gauge). A schematic of the gasifier is shown in Figure 1. The lower stage, operating in a temperature range of 1810 to 1920K (2800° to 3000°F), provides the heat necessary, by partial combustion of char, for the endothermic coal gasification reactions in the upper stage, operating at about 1260K (1800°F). The char is produced from devolatilization of the coal particles injected into the upper stage and consists mainly of fixed carbon and ash contained in the feed coal. The char is entrained by the upward flow through the second stage of the gasifier and passes through the overhead line where it is removed by cyclones. The char that enters the first (lower) stage of the gasifier, therefore, has its origin in the coal feed to the upper stage but enters the lower stage through a recycle line downstream of the cyclones.

The lower stage operates in a slugging mode. Slag removal is achieved by the centrifugal forces of the vortex flow field in the lower stage. The slag is thrown to and accumulates along the walls of the lower stage where gravity drainage permits removal at the bottom in a slag quench vessel. The necessary vortex motion is produced by the orientation of the jets issuing from the steam, air, and char injection nozzles. The main purpose of the vortex flow pattern is to separate the heavier molten slag from the lighter reacting char and to mini-

mize slag carry-over into the upper stage. However, the vortex flow field also promotes mixing and uniform distribution of the particle laden flow and therefore stabilizes the combustion and chemical reactions in the gasifier.

MATHEMATICAL APPROACH

In order to separate important and unimportant scaling criteria in a system complicated by interrelated sets of partial differential equations for the fluid and particle mechanics in the gasifier, an order of magnitude analysis was applied to these equations. For successful application of this technique, it is necessary to nondimensionalize the variables in the equations in such a way as to arrive at dimensionless variables and derivatives whose order of magnitude is around one. Appropriate definition of characteristic values is often dictated by the geometry of the boundaries and physical constraints. The appropriately scaled dimensionless variables and derivatives now of order one by definition will have parametric multipliers which characterize the importance and magnitude of the entire dimensionless term. Substitution of the numerical values of the parametric multipliers can, for a given system, determine the important terms and the corresponding important parameters. If similarity between the system at hand and another system is desired, the important parameters can be combined to determine scaling criteria.

In a symmetrical cylindrical system like the entrained flow gasifier, circumferential gradients are absent, and it is not necessary to define a characteristic angle such that the dimensionless angle is of order unity. Choice of a characteristic radial distance, the gasifier radius, and a characteristic axial distance, the gasifier length, are easily made to produce dimensionless coordinates of order unity. The characteristic time for the flow is taken as the residence time in the gasifier. This need not be a unique quantity but can be defined as the characteristic length divided by a characteristic axial velocity. Therefore, dimensionless independent variables are given by

$$r^* = \frac{r}{R}, \quad z^* = \frac{z}{L}, \quad t^* = \frac{tV_{zc}}{L} \quad (1)$$

The definition of dimensionless dependent variables can be handled initially by arbitrarily assuming the exist-

ence of characteristic radial, circumferential, and axial velocities for the gas. If the particles are small and have low terminal settling velocities and therefore low slip velocities, the characteristic gas velocities can also be used to scale the radial, circumferential, and axial components of the particle velocity. Pressures can be scaled by heads in a similar manner as in the definition of the Euler number. Density differences, considered in buoyancy force terms, require the definition of a characteristic density and dimensionless variable density. Therefore, dimensionless dependent variables are given by

$$V_r^* = \frac{V_r}{V_{rc}}; \quad V_\theta^* = \frac{V_\theta}{V_{\theta c}}; \quad V_z^* = \frac{V_z}{V_{zc}}; \quad \Delta P^* = \frac{P - P_o}{\rho_o V_{zc}^2 / 2g_o} \quad (2)$$

$$u_r^* = \frac{u_r}{V_{rc}}; \quad u_\theta^* = \frac{u_\theta}{V_{\theta c}}; \quad u_z^* = \frac{u_z}{V_{zc}}; \quad \rho^* = \frac{\rho}{\rho_o}$$

The relative particle velocity can be scaled by the Stokes settling velocity. Therefore, the dimensionless relative particle velocity can be defined by

$$u_f^* = \frac{u_f}{u_t}; \quad u_{fr}^* = \frac{u_{fr}}{u_t}; \quad u_{f\theta}^* = \frac{u_{f\theta}}{u_t}; \quad u_{fz}^* = \frac{u_{fz}}{u_t} \quad (3)$$

With the possible exception of the pressure, all of the dimensionless variables are of order unity.

CHARACTERISTIC VELOCITIES

For a given geometry, all three characteristic velocities are simple multiples of each other and are related by the swirl number S . The characteristic circumferential velocity is obtained from the steady state form of the moment-of-momentum equation. Refer to Figures 2 and 3 for the definition of geometrical parameters.

Assuming that the wall shear stress does not significantly affect the circumferential momentum of the flow, the transfer of circumferential momentum from the jet nozzle entrance at the outer periphery of the gasifier to the gasifier itself can be expressed as

$$\dot{m}RV_n \sin\alpha \cos\beta = \dot{m}r_c V_{\theta c} \quad (4)$$

where $r_c \propto$ the average of the flame circle radius and the outer radius. Defining the flame circle radius as the radius of the circle struck tangentially by undeflected jets from the nozzles, the characteristic circumferential vel-

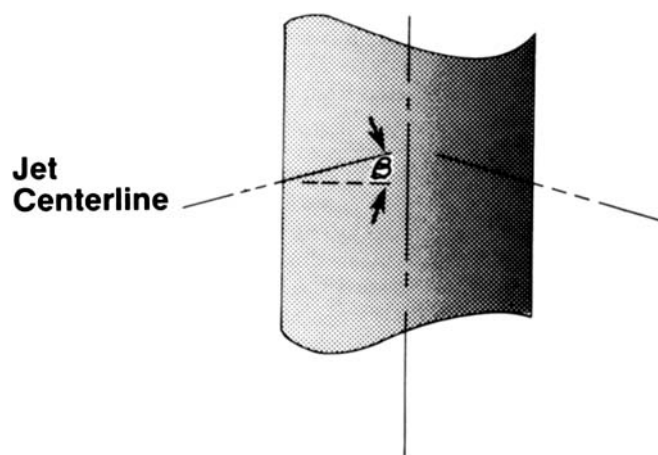
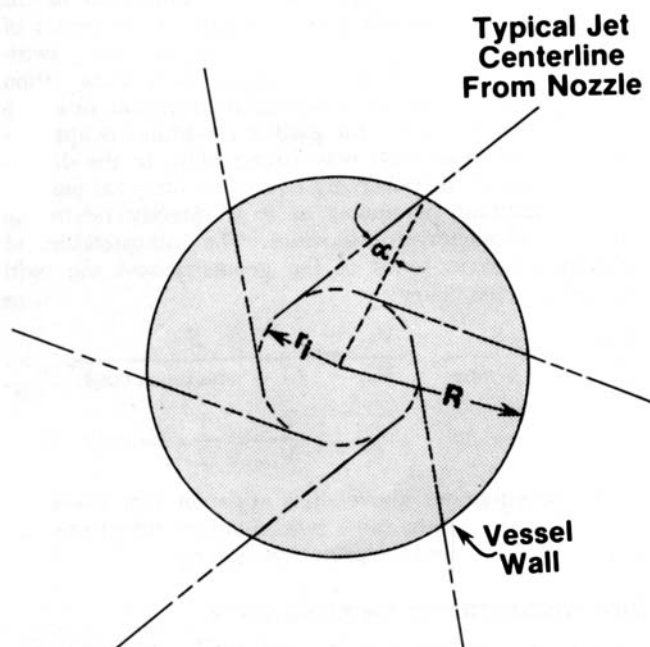


Fig. 3. Nozzle geometry schematic elevation.

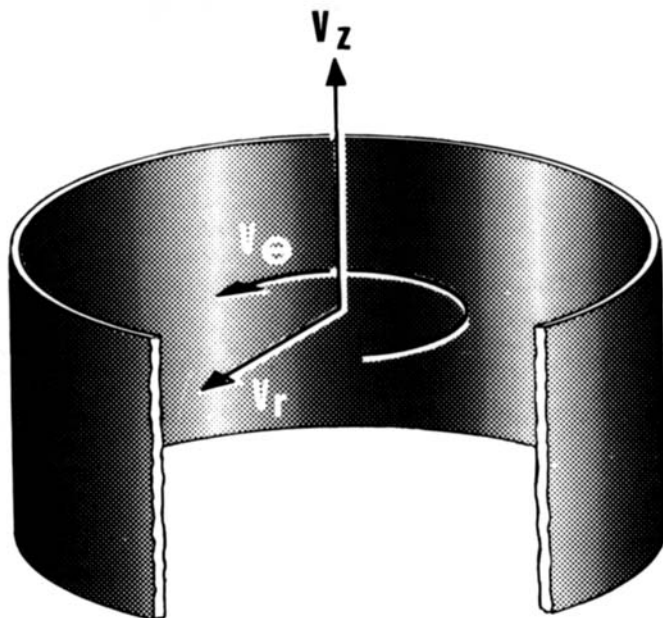


Fig. 4. Velocity components.

ocity is given by

$$V_{\theta c} = V_n \frac{2 \sin \alpha}{1 + \sin \alpha} \cos \beta \quad (5)$$

The characteristic axial velocity is obtained from the mass flow rate of gas leaving the gasifier and the gasifier geometry:

$$V_{zc} = \frac{\dot{m}}{\rho_o \pi R^2} \quad (6)$$

For a test model without reactions, the gaseous mass flow entering through the nozzles will equal the gaseous mass flow leaving the gasifier. This will not generally be true for a reacting system generating additional moles of gas from a solid. However, for an air charged, low British thermal unit coal gasification system, equality of the gas flows is a reasonable approximation for an order of magnitude analysis. Then

$$\dot{m} = \rho_o V_{zc} \pi R^2 \approx \rho_o V_n n_n \pi R_n^2 \quad (7)$$

and

$$V_{zc} = V_n \frac{n_n R_n^2}{R^2} \quad (8)$$

Finally, the characteristic radial velocity can be expressed as the radial component of the mass flow entering through the nozzles divided by the larger flow area of the gasifier. This definition assumes that the radial flow can be represented as part of a vortex system oriented perpendicular to the main vortex (velocity components are shown in Figure 4). Therefore, the characteristic radial velocity is estimated from

$$V_{rc} = \frac{V_n}{2} \frac{n_n R_n^2}{R^2} \cos \alpha \cos \beta \quad (9)$$

The factor $\frac{1}{2}$ has been introduced to account for the fact that the flow gradually turns away from the radial direction toward the axial direction as the remainder of the jet penetrates toward the core. The radial velocity is therefore not uniform across the radius.

Since all the characteristic velocities are related to the nozzle velocity, they are not independent and can be related to each other through geometric factors. For one reported series of tests for a nonreactive system (Smith, 1976), the following values

$$R = 0.30 \text{ m (1 ft)}; \quad R_n = 0.051 \text{ m (0.166 ft)}; \quad n_n = 6$$

$$\alpha \approx 31.7 \text{ deg}; \quad \beta \approx 10 \text{ deg}; \quad V_n \approx 5.8 \text{ m/s (19 ft/s)} \quad (10)$$

give

$$V_{\theta c} = 3.90 \text{ m/s (12.8 ft/s)}; \quad V_{zc} = 0.957 \text{ m/s (3.14 ft/s)}; \\ V_{rc} = 0.396 \text{ m/s (1.3 ft/s)} \quad (11)$$

These values are favorably compared with the characteristic values obtained by inspection of the velocity profiles reported in the same reference. These values, approximately 3.05 m/s (10 ft/s), 0.76 m/s (2.5 ft/s), and 0.30 m/s (1 ft/s) for $V_{\theta c}$, V_{zc} , and V_{rc} , respectively, are in almost exactly the same proportion as the calculated values.

SWIRL NUMBER

The swirl number is defined by Beer and Chigier (1972) for combustor systems as

$$S = \frac{G_\theta}{G_z R} \quad (12)$$

where

$$G_\theta = \int_0^R r V_{\theta c} \rho V_{zc} 2\pi r dr \quad (13)$$

and

$$G_z = \int_0^R V_{zc} \rho V_{zc} 2\pi r dr + \int_0^R g_o P 2\pi r dr \quad (14)$$

Since the swirl number is a comparison of the circumferential momentum in the flow to the axial momentum, it is convenient to redefine these quantities for the gasifier as

$$G_\theta \approx \int_0^R r_c V_{\theta c} \rho V_{zc} 2\pi r dr = \dot{m} r_c V_{\theta c} \quad (15)$$

$$G_z \approx \int_0^R V_{zc} \rho V_{zc} 2\pi r dr = \dot{m} V_{zc} \quad (16)$$

and

$$S \approx \frac{r_c V_{\theta c}}{R V_{zc}} = (1 + \sin \alpha) \frac{V_{\theta c}}{V_{zc}} = \frac{2R^2}{n_n R_n^2} \sin \alpha \cos \beta \quad (17)$$

Equation (17) indicates that the swirl number for the gasifier is a function of the geometry only. The swirl number is largest for jets that enter tangential to the wall and is zero for jets aimed directly at the center of the gasifier. According to Beer and Chigier, strong swirling flows, S greater than 0.6, provide flame stabilization and promote mixing in a recirculation region near the core. The swirl number for gasifier conditions is approximately 6 and represents very strong swirl. In the dimensionless form of the governing equations, the swirl number is an important parameter as it is directly related to ratios of characteristic velocities. The interpretation of velocity ratios in terms of the geometry and the swirl number is given below:

$$\frac{V_{\theta c}}{V_{zc}} = \frac{S}{1 + \sin \alpha}; \quad \frac{V_{\theta c}}{V_{rc}} = \frac{S}{(1 + \sin \alpha) \cos \alpha \cos \beta}; \\ \frac{V_{rc}}{V_{zc}} = \frac{1}{2} \cos \alpha \cos \beta \quad (18)$$

From the equations above, it is apparent that kinematic similitude requires the same swirl number and jet orientation in the model and the prototype systems.

EDDY VISCOSITIES IN SWIRLING FLOW

Evaluation of the turbulent terms in the governing equations necessitated estimation of the order of mag-

nitude of the six independent components of the eddy viscosity tensor. These can be developed from estimates of relative turbulent intensities from linear flows and extrapolation to swirling flows. A reasonable assumption for shear flow in pipes is that the relative turbulence intensity is of the order of 10 to 30% of the mean flow velocity in the most important directions. Further, it was assumed that the fluctuating velocity components in all directions are of the same order of magnitude but are about twice as large in the main flow directions (axial and circumferential) as in the minor flow direction (radial).

The Reynolds stress components in cylindrical coordinates can be related to mean velocity gradients through the eddy viscosity components. For the assumed circumferential symmetry

$$\begin{aligned}\sigma_{rr'} &= -\frac{\rho}{g_0} \overline{v_r'^2} = 2 \frac{\mu_{rr}}{g_0} \frac{\partial V_r}{\partial r} \\ \sigma_{\theta\theta'} &= -\frac{\rho}{g_0} \overline{v_\theta'^2} = 2 \frac{\mu_{\theta\theta}}{g_0} \frac{V_r}{r} \\ \sigma_{zz'} &= -\frac{\rho}{g_0} \overline{v_z'^2} = 2 \frac{\mu_{zz}}{g_0} \frac{\partial V_z}{\partial z} \\ \sigma_{r\theta'} &= \sigma_{\theta r'} = -\frac{\rho}{g_0} \overline{v_r' v_\theta'} = \frac{\mu_{r\theta}}{g_0} \left[r \frac{\partial}{\partial r} \left(\frac{V_\theta}{r} \right) \right] \\ \sigma_{zr'} &= \sigma_{rz'} = -\frac{\rho}{g_0} \overline{v_r' v_z'} = \frac{\mu_{zr}}{g_0} \left(\frac{\partial V_r}{\partial z} + \frac{\partial V_z}{\partial r} \right) \\ \sigma_{\theta z'} &= \sigma_{z\theta'} = -\frac{\rho}{g_0} \overline{v_\theta' v_z'} = \frac{\mu_{\theta z}}{g_0} \left(\frac{\partial V_\theta}{\partial z} \right)\end{aligned}$$

If we use characteristic values from reported data (Smith, 1976) and conservatively high estimates for turbulence intensities (Hinze, 1959) the order of magnitude of the eddy viscosity components is estimated:

$$\begin{aligned}\mu_{rr} &= -\frac{\rho_0 V_{rc} R}{2} \left(\frac{\overline{v_r'^2}}{V_{rc}^2} \right) \frac{\rho^*}{(\partial V_r^* / \partial r^*)} \\ &= o \left[0.0521 \frac{\text{kg}}{\text{m-s}} \left(0.035 \frac{\text{lb m}}{\text{ft-s}} \right) \right] \\ \mu_{\theta\theta} &= -\frac{\rho_0 V_{\theta c}^2 R}{2 V_{rc}} \left(\frac{\overline{v_\theta'^2}}{V_{\theta c}^2} \right) \frac{\rho^* r^*}{V_r^*} \\ &= o \left[0.326 \frac{\text{kg}}{\text{m-s}} \left(0.219 \frac{\text{lb m}}{\text{ft-s}} \right) \right] \\ \mu_{zz} &= -\frac{\rho_0 V_{zc} L}{2} \left(\frac{\overline{v_z'^2}}{V_{zc}^2} \right) \frac{\rho^*}{(\partial V_z^* / \partial z^*)} \\ &= o \left[1.30 \frac{\text{kg}}{\text{m-s}} \left(0.875 \frac{\text{lb m}}{\text{ft-s}} \right) \right] \\ \mu_{r\theta} &= -\rho_0 V_{rc} R \left(\frac{\overline{v_r' v_\theta'}}{V_{rc} V_{\theta c}} \right) \frac{\rho^*}{\left(\frac{\partial V_\theta^*}{\partial r^*} - \frac{V_\theta^*}{r^*} \right)} \\ &= o \left[0.0261 \frac{\text{kg}}{\text{m-s}} \left(0.0175 \frac{\text{lb m}}{\text{ft-s}} \right) \right] \\ \mu_{rz} &= -\rho_0 V_{rc} V_{zc} \left(\frac{\overline{v_r' v_z'}}{V_{rc} V_{zc}} \right) \rho^* / \end{aligned}$$

$$\begin{aligned}& \left(\frac{V_{rc}}{L} \frac{\partial V_r^*}{\partial z^*} + \frac{V_{zc}}{R} \frac{\partial V_z^*}{\partial r^*} \right) \\ &= o \left[0.100 \frac{\text{kg}}{\text{m-s}} \left(0.067 \frac{\text{lb m}}{\text{ft-s}} \right) \right]\end{aligned}$$

$$\begin{aligned}\mu_{z\theta} &= -\rho_0 V_{zc} L \left(\frac{\overline{v_\theta' v_z'}}{V_{\theta c} V_{zc}} \right) \frac{\rho^*}{(\partial V_\theta^* / \partial z^*)} \\ &= o \left[0.655 \frac{\text{kg}}{\text{m-s}} \left(0.44 \frac{\text{lb m}}{\text{ft-s}} \right) \right]\end{aligned} \quad (20)$$

The trends of these results correspond exactly to those reported by Beer and Chigier (1972) for swirling flow in a combustor. No other source of confirming data is available.

VORTEX EQUATIONS OF MOTION

In the general case, the radial, circumferential, and axial equations of motion for a turbulent, incompressible swirling flow carrying suspended particles are given by

$$\begin{aligned}\rho \left(\frac{\partial V_r}{\partial t} + V_r \frac{\partial V_r}{\partial r} + V_z \frac{\partial V_r}{\partial z} - \frac{V_\theta^2}{r} \right) &= -g_0 \frac{\partial P}{\partial r} \\ &+ \mu \left(\frac{1}{r} \frac{\partial}{\partial r} \left(r \frac{\partial V_r}{\partial r} \right) + \frac{\partial^2 V_r}{\partial z^2} - \frac{V_r}{r^2} \right) - \frac{\rho}{r} \frac{\partial}{\partial r} (\overline{r v_r'^2}) \\ &- \rho \frac{\partial}{\partial z} (\overline{v_r' v_z'}) - \rho \frac{\overline{v_\theta'^2}}{r} - \frac{n_p C_d A \rho u_f u_{fr}}{2}\end{aligned} \quad (21)$$

$$\begin{aligned}\rho \left(\frac{\partial V_\theta}{\partial t} + V_r \frac{\partial V_\theta}{\partial r} + V_z \frac{\partial V_\theta}{\partial z} + \frac{V_r V_\theta}{r} \right) &= \mu \left(\frac{1}{r} \frac{\partial}{\partial r} \left(r \frac{\partial V_\theta}{\partial r} \right) + \frac{\partial^2 V_\theta}{\partial z^2} - \frac{V_\theta}{r^2} \right) - \rho \frac{\rho}{\partial r} (\overline{v_\theta' v_r'}) \\ &- \rho \frac{\partial}{\partial z} (\overline{v_\theta' v_z'}) - 2\rho \frac{\overline{v_\theta' v_r'}}{r} - \frac{n_p C_d A \rho u_f u_{f\theta}}{2}\end{aligned} \quad (22)$$

$$\begin{aligned}\rho \left(\frac{\partial V_z}{\partial t} + V_r \frac{\partial V_z}{\partial r} + V_z \frac{\partial V_z}{\partial z} \right) &= -g_0 \frac{\partial P}{\partial z} \\ &+ \mu \left(\frac{1}{r} \frac{\partial}{\partial r} \left(r \frac{\partial V_z}{\partial r} \right) + \frac{\partial^2 V_z}{\partial z^2} \right) - \rho \frac{\overline{\partial v_z'^2}}{\partial z} \\ &- \frac{\rho}{r} \frac{\partial}{\partial r} (\overline{r v_r' v_z'}) - \frac{1}{2} n_p C_d A \rho u_f u_{fz} \\ &+ \rho_0 g [1 + \beta_0 (T - T_0)]\end{aligned} \quad (23)$$

Since the procedure for nondimensionalizing the equations and evaluating them is quite lengthy, the treatment of the radial equation will be used to demonstrate the procedure. For the other equations and the particle equations of motion described later, the procedure is similar. For these equations, only the general equation, the final simplified equation, and a summary of the order of magnitude for each equation will be given.

The order of magnitude analysis is based mainly on the geometry and the conditions in an air blown gasifier. Two values of density were used depending on which one was conservative or compatible with the other data in the term or equation. Since the vortex flow tests were operated at low temperature without particles, the lower value of density was used to evaluate the eddy viscosity and terms in the vortex equation of motion, using the cold

TABLE 1. PARTICLE PROPERTIES

	Coal	Char
Typical diameter	45 μm (0.000148 ft)	170 μm (0.000508 ft)
Loading density	$1.39 \times 10^{10} \frac{\text{particles}}{\text{m}^3} \left(3.93 \times 10^8 \frac{\text{particles}}{\text{ft}^3} \right)$	$4.8 \times 10^8 \frac{\text{particles}}{\text{m}^3} \left(1.37 \times 10^7 \frac{\text{particles}}{\text{ft}^3} \right)$
Density of a particle	$2400 \frac{\text{kg}}{\text{m}^3}$ (150 lb m/ft ³)	$640 \frac{\text{kg}}{\text{m}^3}$ (40 lb m/ft ³)
Stokes settling velocity	$0.0668 \frac{\text{m}}{\text{s}}$ (0.219 ft/s)	$0.250 \frac{\text{m}}{\text{s}}$ (0.821 ft/s)
Drag coefficient based on Stokes velocity	60.5	5.52
Relaxation time	0.00679 s	0.0257 s
Settling Reynolds number	0.4	5.8
Cross-sectional area	$1.60 \times 10^{-9} \text{m}^2$ ($1.72 \times 10^{-8} \text{ft}^2$)	$2.28 \times 10^{-7} \text{m}^2$ ($2.45 \times 10^{-7} \text{ft}^2$)

flow test data. A larger value of density was used in the particle equations of motion to account for the high pressure in the gasifier and to conservatively consider particle drag and buoyancy. The results were compatible using either cold flow or hot flow data. The assumed data is summarized below:

$$R = 0.30 \text{ m (1 ft)}; \quad L = 3.05 \text{ m (10 ft)};$$

$$\rho_o = 1.12 \frac{\text{kg}}{\text{m}^3} \left(0.07 \frac{\text{lb m}}{\text{ft}^3} \right) \text{ or } 5.42 \frac{\text{kg}}{\text{m}^3} \left(0.338 \frac{\text{lb m}}{\text{ft}^3} \right);$$

$$\mu = 0.000268 \frac{\text{kg}}{\text{m-s}} \left(0.000180 \frac{\text{lb m}}{\text{ft-s}} \right)$$

$$\text{or } 0.00000400 \frac{\text{kg}}{\text{m-s}} \left(0.00000269 \frac{\text{lb m}}{\text{ft-s}} \right);$$

$$V_{rc} = 0.30 \frac{\text{m}}{\text{s}} \left(1 \frac{\text{ft}}{\text{s}} \right);$$

$$V_{\theta c} = 3.05 \frac{\text{m}}{\text{s}} \left(10 \frac{\text{ft}}{\text{s}} \right)$$

$$V_{zc} = 0.76 \frac{\text{m}}{\text{s}} \left(2.5 \frac{\text{ft}}{\text{s}} \right)$$

(24)

Representative particle properties are summarized in Table 1.

The radial equation of motion, after substitution of the eddy viscosity definitions, introduction of the dimensionless variables, and division by the coefficient of the centrifugal force term becomes

$$\begin{aligned} \rho^* \left(\frac{R}{L} \frac{V_{rc} V_{zc}}{V_{\theta c}^2} \frac{\partial V_r^*}{\partial t^*} + \frac{V_{rc}^2}{V_{\theta c}^2} V_r^* \frac{\partial V_r^*}{\partial r^*} \right. \\ \left. + \frac{R}{L} \frac{V_{rc} V_{zc}}{V_{\theta c}^2} V_z^* \frac{\partial V_r^*}{\partial z^*} - \frac{V_{\theta}^{*2}}{r^*} \right) = - \frac{V_{zc}^2}{V_{\theta c}^2} \frac{\partial P^*}{\partial r^*} \\ - \frac{R}{2} n_p C_d A \frac{u_t^2}{V_{\theta c}^2} \rho^* u_f^* u_{fr}^* + \frac{\mu V_{rc}}{\rho_o R V_{\theta c}^2} \frac{\partial}{\partial r^*} \left(r^* \frac{\partial V_r^*}{\partial r^*} \right) \\ + \frac{\mu R V_{rc}}{\rho_o L^2 V_{\theta c}^2} \frac{\partial^2 V_r^*}{\partial z^{*2}} - \frac{\mu V_{rc} V_r^*}{\rho_o R V_{\theta c}^2 r^{*2}} \\ + \frac{2 V_{rc}}{\rho_o R V_{\theta c}^2} \frac{1}{r^*} \frac{\partial}{\partial r^*} \left(r^* \mu_{rr} \frac{\partial V_r^*}{\partial r^*} \right) - \frac{2 V_{rc}}{\rho_o R V_{\theta c}^2} \mu_{\theta\theta} \frac{V_r^*}{r^{*2}} \\ + \frac{1}{L} \frac{\partial}{\partial z^*} \left[\mu_{rz} \left(\frac{R}{L} \frac{V_{rc}}{\rho_o V_{\theta c}^2} \frac{\partial V_r^*}{\partial z^*} + \frac{V_{zc}}{\rho_o V_{\theta c}^2} \frac{\partial V_r^*}{\partial r^*} \right) \right] \end{aligned} \quad (25)$$

TABLE 2. VORTEX RADIAL EQUATION

Term	Description	Magnitude
I	Unsteady	$o(0.0025)$
II	Inertial-radial gradient	$o(0.01)$
III	Inertial-axial gradient	$o(0.0025)$
IV	Centrifugal force	$o(1)$
V	Pressure gradient	$o(1)$
VI	Particle drag	$o(0.05, 0.1)$ char, coal
VII	Viscous—radial gradient (1 of 2)	$o(0.00000180)$
VIII	Viscous—axial gradient	$o(0.0000000180)$
IX	Viscous—radial gradient (2 of 2)	$o(0.00000180)$
X	Turbulent—radial	$o(0.01)$
XI	Turbulent—circumferential	$o(0.06)$
XII	Turbulent—axial gradient	$o(0.0001)$
XIII	Turbulent—radial gradient	$o(0.0025)$

Table 2 summarizes the order of magnitude of each of the thirteen terms in the radial equation of motion. Note that the order of magnitude of the particle drag term depends on whether coal or char properties are chosen.

If we omit negligible terms, the radial equation of motion is

$$\frac{\rho^* V_{\theta}^{*2}}{r^*} = \frac{V_{zc}^2}{V_{\theta c}^2} \frac{\partial P^*}{\partial r^*} - \frac{R}{2} n_p C_d A \frac{u_t^2}{V_{\theta c}^2} \rho^* u_f^* u_{fr}^* \quad (26)$$

The radial equation, therefore, is a balance between centrifugal, pressure, and particle drag forces. None of the viscous or turbulent terms are important. Table 3 shows the results of the order of magnitude analysis for the circumferential equation of motion.

The simplified circumferential equation of motion is

$$\begin{aligned} \frac{R}{L} \frac{V_{zc}}{V_{rc}} \rho^* \frac{\partial V_{\theta}^*}{\partial t^*} + \rho^* V_r^* \frac{\partial V_{\theta}^*}{\partial r^*} + \frac{R}{L} \frac{V_{zc}}{V_{rc}} \rho^* V_z^* \frac{\partial V_{\theta}^*}{\partial z^*} \\ + \rho^* \frac{V_r^* V_{\theta}^*}{r^*} = - \frac{R}{2} n_p C_d A \frac{u_t^2}{V_{rc} V_{\theta c}} \rho^* u_f^* u_{f\theta}^* \\ + \frac{1}{\rho_o R V_{rc}} \frac{\partial}{\partial r^*} \left[\mu_{r\theta} \frac{\partial}{\partial r^*} \left(\frac{V_{\theta}^*}{r^*} \right) \right] \\ + \frac{2}{\rho_o R V_{rc}} \left[\mu_{r\theta} \frac{\partial}{\partial r^*} \left(\frac{V_{\theta}^*}{r^*} \right) \right] \end{aligned} \quad (27)$$

The only terms that are certainly unimportant are the viscous terms. If the vessel radius is increased significantly, the two eddy viscosity terms may lose their significance,

TABLE 3. VORTEX CIRCUMFERENTIAL EQUATION

Term	Description	Magnitude
I	Unsteady	$o(0.25)$
II	Inertial—radial gradient	$o(1)$
III	Inertial—axial gradient	$o(0.25)$
IV	Coriolis	$o(1)$
V	Particle drag	$o(0.5, 1)$ char, coal
VI	Viscous—radial gradient (1 of 2)	$o(0.000180)$
VII	Viscous—axial gradient	$o(0.0000180)$
VIII	Viscous—radial gradient (2 of 2)	$o(0.000180)$
IX	Turbulent—radial gradient (1 of 2)	$o(0.25)$
X	Turbulent—axial gradient	$o(0.06)$
XI	Turbulent—radial gradient (2 of 2)	$o(0.5)$

while other terms (particularly if the length is not increased proportionately) may gain significance. The only eddy viscosity term that has been omitted, term X, would then have to be reevaluated.

Table 4 summarizes the order of magnitude analysis for the axial equation of motion.

The final form of the axial equation of motion is

$$\begin{aligned} \frac{R}{L} \frac{V_{zc}}{V_{rc}} \rho^* \frac{\partial V_z^*}{\partial t^*} + \rho^* V_r^* \frac{\partial V_z^*}{\partial r^*} + \frac{R}{L} \frac{V_{zc}}{V_{rc}} \rho^* V_z^* \frac{\partial V_z^*}{\partial z^*} \\ = - \frac{R}{L} \frac{V_{zc}}{V_{rc}} \frac{\partial P^*}{\partial z^*} + \frac{gR}{V_{rc} V_{zc}} + \frac{gR}{V_{rc} V_{zc}} \beta_0 (T - T_0) \\ - \frac{R}{2} n_p C_d A \frac{u_t^2}{V_{rc} V_{zc}} \rho^* u_f^* u^* f_z \\ + \frac{2R}{\rho_0 L^2 V_{rc}} \frac{\partial}{\partial z^*} \left(\mu_{zz} \frac{\partial V_z^*}{\partial z^*} \right) \\ + \frac{1}{\rho_0 V_{rc} R r^*} \frac{\partial}{\partial r^*} \left(r^* \mu_{rz} \frac{\partial V_z^*}{\partial r^*} \right) \quad (28) \end{aligned}$$

The buoyancy force will be significant if temperature differences of 55°K (100°R) or more are possible in the gasifier. This term accounts for the effect of gas compressibility without having to resort to the use of compressible flow equations.

PARTICLE EQUATIONS OF MOTION

The particle equations of motion for the radial, circumferential, and axial direction are described in the La Grangian sense of following the motion of an individual particle:

$$\begin{aligned} \frac{m}{g_0} \frac{du_r}{dt} - \frac{m}{g_0} \frac{u_\theta^2}{r} + \frac{u_r}{g_0} \frac{dm}{dt} = C_p A \rho \frac{u_f u_{fr}}{g_0} \\ + \frac{m}{\rho_s} \frac{\rho}{g_0} \frac{V_\theta^2}{r} + \frac{m \rho_{ds}}{2 \epsilon_0} \left(\frac{q}{m} \right)^2 r + F_{thr} + F_{mr} \quad (29) \end{aligned}$$

$$\frac{m}{g_0} \frac{du_\theta}{dt} + \frac{m}{g_0} \frac{u_r u_\theta}{r} + \frac{u_\theta}{g_0} \frac{dm}{dt} = C_D A \frac{\rho u_f u_{f\theta}}{2 g_0} \quad (30)$$

$$\begin{aligned} \frac{m}{g_0} \frac{du_z}{dt} + \frac{u_z}{g_0} \frac{dm}{dt} = C_D A \frac{\rho u_f u_{fz}}{2} \\ + \frac{\rho}{\rho_s} m \frac{g}{g_0} - m \frac{g}{g_0} + \frac{m}{\rho_s} \frac{\partial P}{\partial z} \quad (31) \end{aligned}$$

TABLE 4. VORTEX AXIAL EQUATION

Term	Description	Magnitude
I	Unsteady	$o(0.25)$
II	Inertial—radial gradient	$o(1)$
III	Inertial axial gradient	$o(0.25)$
IV	Pressure gradient	$o(0.25)$
V	Gravity	$o(10)$
VI	Buoyancy	$o(1)$
VII	Particle drag	$o(1.9, 3.8)$ char, coal
VIII	Viscous—radial gradient	$o(0.000180)$
IX	Viscous—axial gradient	$o(0.0000180)$
X	Turbulent—axial	$o(0.25)$
XI	Turbulent—axial gradient	$o(0.038)$
XII	Turbulent—radial gradient	$o(1)$

TABLE 5. PARTICLE RADIAL EQUATION

Term	Description	Magnitude
I	Radial acceleration	$o(0.0025)$
II	Centrifugal force	$o(1)$
III	Mass reaction	$o(0.0075)$
IV	Fluid drag	$o(0.322)$
V	Radial pressure	$o(0.002, 0.008)$ coal, char
VI	Electrostatic charge	$o(0.0044)$
VII	Thermophoresis	$o(0.0006)$
VIII	Magnus force	$o(0.01)$

TABLE 6. PARTICLE CIRCUMFERENTIAL EQUATION

Term	Description	Magnitude
I	Circumferential acceleration	$o(0.25)$
II	Coriolis acceleration	$o(1)$
III	Mass reaction	$o(0.75)$
IV	Fluid drag	$o(3.22)$

TABLE 7. PARTICLE AXIAL EQUATION

Term	Description	Magnitude
I	Axial acceleration	$o(1)$
II	Mass reaction	$o(3)$
III	Fluid drag	$o(52)$
IV	Particle buoyancy	$o(0.43)$
V	Particle weight	$o(52)$
VI	Axial pressure	$o(0.008)$

The radial equation, in the general case, includes terms accounting for electrostatic charging, thermophoresis, and magnus forces. These forces are absent from the circumferential equation because of the assumed symmetry of the flow field. More important forces than these in the vertical direction (particle buoyancy, weight, and vertical pressure gradient) have been added to the axial equation. The electrostatic, thermophoresis, and magnus forces were estimated from expressions given by Boothroyd (1971) and by Soo (1967). Tables 5, 6, and 7 summarize the relative orders of magnitude of the terms in the radial, circumferential, and axial equations of motion, respectively.

The simplified equations of motion, neglecting the radial acceleration, radial mass reaction, radial and axial pressure, electrostatic, thermophoresis, magnus, and particle buoyancy forces are

TABLE 8. SIGNIFICANT DIMENSIONLESS GROUPS

Group	Interpretation	Source
R/L	Overall geometric scale ratio	Particle, vortex equations of motion
S	Swirl number; nozzle orientation and geometry	Particle, vortex equations of motion
V_{zc}^2/gL	Froude number	Particle, vortex equations of motion
ρ_{ds}/ρ_o	Particle loading ratio	Vortex equations of motion
$\frac{gR}{V_{rc}V_{zc}}\beta_o(T-T_o)$	Buoyancy-gravity comparison	Vortex equations of motion
$\frac{V_r V_{\theta c}}{v_r' v_{\theta}'}$	Local turbulent scales	Vortex equations of motion
$\frac{H_c}{C_p \Delta T_c} \frac{H_{cs}}{C_{ps} \Delta T_{cs}}$	Heat of reaction—heat capacity comparison	Vortex, particle energy equations
Bi	Biot modulus	Particle energy equation
$\frac{K''' L}{V_{zc}}$	Reaction-residence time comparison	Gas species equation

$$-\frac{u_{\theta}^{*2}}{r^*} = \frac{3}{4} C_D \frac{R}{d_o} \frac{\rho_o}{\rho_s} \frac{u_t^2}{V_{\theta c}^2} \frac{\rho^*}{d^*} u_f^* u_{fr}^* \quad (32)$$

$$\begin{aligned} \frac{R}{L} \frac{V_{zc}}{V_{rc}} \frac{du_{\theta}^*}{dt^*} + \frac{u_r^* u_{\theta}^*}{r^*} + \frac{R}{L} \frac{V_{zc}}{V_{rc}} \frac{3}{d^*} \frac{dd^*}{dt^*} \\ = \frac{3}{4} C_D \frac{R}{d_o} \frac{\rho_o}{\rho_s} \frac{u_t^2}{V_{cr} V_{\theta c}} \frac{\rho^*}{d^*} u_f^* u_{f\theta}^* \end{aligned} \quad (33)$$

$$\frac{du_z^*}{dt^*} + \frac{3}{d^*} \frac{dd^*}{dt^*} = \frac{3}{4} C_D \frac{L}{d_o} \frac{\rho_o}{\rho_s} \frac{u_t^2}{V_{zc}^2} \frac{\rho^*}{d^*} u_f^* u_{fz}^* - \frac{Lg}{V_{zc}^2} \quad (34)$$

where d^* , a dimensionless particle diameter based on d_o , has been introduced.

SIGNIFICANT DIMENSIONLESS GROUPS AND SCALING

The simplified forms of the vortex and particle equations of motion contain dimensionless groups that can be combined to produce the scaling laws for the gasifier. The most significant groups are summarized in Table 8. For completeness, significant groups based on a similar analysis that appear in the gas species equation, vortex energy equation, and particle energy equation are also listed. If the particle drag parameters are recast in a more easily interpretable form by reasoning that the size of the deviations from Stokes flow formula are not great enough to invalidate an order of magnitude analysis based on Stokes flow formulas, the particle drag terms become independent of particle properties.

The Reynolds number and Mach number are absent from Table 8 since they are not important for scaling. If the turbulence intensities are controlled by an invariant local structure (Hinze, 1959), the turbulent Reynolds type of numbers based on eddy viscosity will also be invariant. Only gross changes in the geometry and Froude number would affect this invariance. Therefore, Reynolds numbers based on molecular or turbulent eddy viscosities, provided the Reynolds numbers are high, have little or no effect on the flow.

Matching of the energy groups from model to prototype should not be difficult, since the intention will probably be to maintain the same temperature and reactions. Because overall thermal similarity appears to be possible, it appears that kinematic similarity is also possible as the two are related through the buoyancy term. The groups deemed important from the equations of motion can therefore be combined into the scaling rules summarized in the conclusions.

ACKNOWLEDGMENT

The authors are grateful to the Energy Research and Development Administration, Empire State Electric Research Council, General Electric Gas Turbine Division, Northern States Power Company, and the Foster Wheeler Energy Corporation for their joint sponsorship under ERDA contract number 14-32-0001-1521. The consultation and original coal gasification development work by Bituminous Coal Research, Inc., is gratefully appreciated.

NOTATION

A	= frontal cross-sectional area of a particle
Bi	= Biot modulus
C_D	= drag coefficient of a particle based on μ_f
C_p	= specific heat
d_o	= initial or characteristic particle diameter
F_{mr}	= radial magnus force
F_{thr}	= radial thermophoresis force
g	= gravitational acceleration
g_o	= gravitational constant
G_z	= axial flow of momentum
G_{θ}	= circumferential flow of moment-of-momentum
H_c	= characteristic heat of reaction
K'''	= reaction rate constant
L	= characteristic length of the gasifier
m	= mass of a particle
\dot{m}	= characteristic gas mass flow rate
n_n	= number of nozzles
n_p	= number of particles per unit volume
P	= gasifier pressure
P_o	= reference gas pressure
q	= charge on a particle
r	= radial coordinate from gasifier axis
r_c	= characteristic radius for circumferential momentum
r_i	= flame circle radius
R	= radius of gasifier cylinder
R_n	= nozzle radius
S	= swirl number, circumferential to axial momentum ratio
t	= time
T	= gas temperature
T_o	= reference gas temperature
u	= total particle velocity
u_t	= Stokes settling velocity
u_r, u_{θ}, u_z	= components of particle velocity vector
v_r, v_{θ}, v_z	= fluctuating components of gas velocity
V_r, V_{θ}, V_z	= components of gas velocity vector-local mean values
V_n	= nozzle velocity
z	= axial distance along gasifier

Greek Letters

- α = jet angle with radius in a horizontal plane
 β = jet angle with wall in a vertical plane
 β_o = temperature coefficient of volume expansion at T_o
 ϵ_o = electrostatic permittivity
 θ = circumferential angle
 μ = gas viscosity
 $\mu_{rr}, \mu_{\theta\theta}$, etc. = components of eddy viscosity tensor
 ρ = density of suspending gas
 ρ_{ds} = density of dispersed solids
 ρ_o = characteristic average gas density
 ρ_s = density of solid particle
 $\sigma_{rr}, \sigma_{\theta\theta}$, etc. = components of Reynolds stress tensor

Subscripts

- c = characteristic value
 f = relative to the gas velocity
 n = nozzle
 r = radial component
 s = solid particle
 z = axial component
 θ = circumferential component

Superscripts and Symbols

- * = dimensionless value
— = temporal or ensemble average
 o = order of magnitude given in parentheses

LITERATURE CITED

- Anon., "Gas Generator Research and Development," Survey and Evaluation, Phase One, Volume One, BCR Report L-156, Office of Coal Research, Department of the Interior, Washington, D.C. (Mar., 1965).
Beer, J. M., and N. A. Chigier, *Combustion Aerodynamics*, Applied Science Publishers, Ltd., London, England (1972).

- Boothroyd, R. G., *Flowing Gas-Solids Suspensions*, Chapman and Hall, Ltd., London, England (1971).
Donath, E. E., U.S. Patent 3,732,913, "Two Stage Gasification of Coal With Forced Reactant Mixing and Steam Treatment of Recycled Char," (Jan. 1, 1974).
Elliot, M. A., et al., "Gasification of Pulverized Coal with Oxygen and Steam in a Vortex Reactor," *Ind. Eng. Chem.*, 44, 1074 (1952).
Hinze, J. O., *Turbulence, an Introduction to Its Mechanism and Theory*, McGraw-Hill, New York (1959).
Hull, D. E., "Status of the Bi-Gas Coal Gasification Pilot Plant," Proceedings of the Seventh Synthetic Pipeline Gas Symposium, American Gas Association, Chicago, Ill. (1975).
McCallister, R. A., and G. C. Ashley, "Coal Gasification to Produce Low Btu Fuel for Combined Cycle Power Generation," American Power Conference, Chicago, Ill. (1974).
Shapiro, A. H., *The Dynamics and Thermodynamics of Compressible Fluid Flow*, Vol. I, The Ronald Press Company, New York (1953).
Smith, D. E., *Development Work for an Advanced Coal Gasification System for Electric Power Generation from Coal Directed Toward a Commercial Gasification Generating Plant, Phase II, Monthly Technical Progress Report, January 1976*, ERDA report No. FE-1521-12, Foster Wheeler Energy Corporation, Livingston, N.J. (1976).
Smoot, L. D., and R. W. Hanks, "The Influence of Mixing on Kinetic Processes in Entrained Coal Gasifiers," Quarterly Technical Progress Report No. 1, ERDA Contract No. 14-32-0001-1767 (1975).
Soo, S. L., *Fluid Dynamics of Multiphase Systems*, Blaisdell Publishing, Waltham, Mass. (1967).
Zahradnik, R. L., and R. J. Grace, "Chemistry and Physics of Entrained Coal Gasification," *Coal Gasification*, L. G. Massey, ed., Chapt. 9, Advances in Chemistry Series 131, Symposium sponsored by Division of Fuel Chemistry, 165th meeting of the American Chemical Society, Dallas, Tex. (Apr. 9-10, 1973).

Manuscript received February 17; revision received August 25, and accepted September 14, 1977.

Aeration and Mixing in Deep Tank Fermentation Systems

MELBOURNE L. JACKSON

and

CHIA-CHEUH SHEN

Department of Chemical Engineering
University of Idaho
Moscow, Idaho 83843

Oxygen transfer characteristics for three sizes of equipment, from 76 mm to 7.6 m in diameter and for liquid depths from 4 to 21 m, correlate well and permit scaling of fermentation systems in size. Simple orifice inlets for gas flow, uniformly distributed over a tank bottom, effect rapid mixing and permit very high oxygen demands to be met. Supersaturation provides dissolved gases for the flotation and solids separation as an inherent processing procedure. Nearly uniform bulk liquid composition and a linear decrease of gas phase composition with depth permit a proper, integrated value of the oxygen saturation driving force to be employed. Results provide the design basis for large scale aeration systems which offer potential savings in both capital and energy.

SCOPE

Large fermentation systems, including wastewater treatment processes, have been handicapped by the characteristics of a high oxygen demand and need for good

mixing, and in some cases by restrictions imposed by a shortage of land. Needed for the design of deep tanks which can meet these requirements is the performance of aeration systems as to type and spacing or aeration devices and predictable mass transfer characteristics under high hydrostatic heads. The trade currently considers deep tanks to be those of 8 to 9 m in height, but greater

Correspondence concerning this paper should be addressed to Melbourne L. Jackson.

0001-1541/78/8493-0063/\$01.15 © 1978, American Institute of Chemical Engineers.